Journal of Polymer Research (2022) 29: 111
https://doi.org/10.1007/s10965-022-02969-9

ORIGINAL PAPER

Donor – acceptor and donor – donor alternating conjugated polymers based on dithieno[3,2-b:2',3'-d]pyrrole: synthesis, optical properties and organic solar cells applications

Duong Thanh Le[1] · Nhung Thanh Thi Truong[1] · Tam Hoang Luu[2] · Le-Thu T. Nguyen[2] · Mai Ha Hoang[3] · Ha Phuong Ky Huynh[4] · Son Thanh Cu[5] · Quoc Thiet Nguyen[5] · Ha Tran Nguyen[1,2]

Received: 23 September 2021 / Accepted: 2 March 2022 / Published online: 4 March 2022

Abstract
In this paper, two novel donor–acceptor (D-A) and donor-donor (D-D) conjugated polymers containing dithieno[3,2-b:2',3'-d]pyrrole in combined respectively with thieno[3,4-c]pyrrole-4,6-dione and benzo[1,2-b:4,5-b']dithiophene derivatives were synthesized successfully via direct (hetero) arylation polymerization where the $Pd(OAc)_2$ and $PCy_3.HBF_4$ have been used as the catalyst system. The obtained conjugated copolymers have been characterized via FT-IR, GPC, ^1H NMR and XRD to determine the chemical structures, chemical compositions as well as the macromolecular characteristic features. In addition the conjugated polymers have been investigated for the optical and thermal properties including UV–Vis, fluorescent emission, DSC and TGA respectively. The electrochemical properties of the conjugated polymers have been evaluated via cyclic voltammetry to determine the HOMO–LUMO energy levels which are suitable for organic solar cells devices.

Keywords Donor–acceptor · Donor-donor conjugated polymers · Dithieno [3,2-b:2',3'-d] pyrrole · Organic solar cells · Direct arylation polymerization

Introduction

In the past decades, plastic solar cells (PSCs) have been one of the options for using renewable clean energy to replace traditional energy sources owing to their excellent properties such as lightweight, low production costs, and flexible devices [1]. Up to now, the power conversion efficiency (PCE) of PSCs has been impressively improved and increased to 18%, obtained from low-energy bandgap materials and innovative device fabrication engineering [2–4]. To achieve the higher PCEs, the crucial challenges are to narrow the energy bandgap of π-conjugated polymers to widen the absorption spectra (larger, J_{sc}) and to lower the highest occupied molecular orbital (HOMO) energy level of conjugated polymers (higher, V_{oc}) [5]. That low-energy bandgap and lowered HOMO energy level are usually obtained by using the alternating donor/acceptor repeating unit strategy in the conjugated polymers backbone [6]. Beside the application of conjugated polymers in organic solar cells and electronic devices, the conjugated polymers were also applied as potential materials in corrosion resistance materials, amperometric sensors and dielectric materials [7–9]

Among the donor units, dithieno [3,2-b:2',3'-d] pyrrole (DTP) is an excellent electron-rich unit showing good π-conjugation and low ionization potential due to a planar tricyclic system and electron-rich nitrogen atom in its structure [10]. However, DTP-based materials usually display high HOMO levels leading to low open-circuit voltages (Voc) and low PCEs [11, 12]. Thus, there have

✉ Ha Tran Nguyen
nguyentranha@hcmut.edu.vn

1 National Key Laboratory of Polymer and Composite Materials, Ho Chi Minh City University of Technology, Vietnam National University–Ho Chi Minh City (VNU–HCM), 268 Ly Thuong Kiet, District 10, Ho Chi Minh City, Vietnam

2 Faculty of Materials Technology, Ho Chi Minh City University of Technology (HCMUT), Vietnam National University, 268 Ly Thuong Kiet, District 10, Ho Chi Minh City, Vietnam

3 Institute of Chemistry, Vietnam Academy of Science and Technology, 18 Viet Hoang Quoc, Ha Noi, Vietnam

4 Faculty of Chemical Engineering, Ho Chi Minh City University of Technology, Vietnam National University (VNU–HCM), 268 Ly Thuong Kiet, District 10, Ho Chi Minh City, Vietnam

5 Institute of Applied Materials Science, Vietnam Academy of Science and Technology, 01 TL29, District 12, Ho Chi Minh City, Vietnam

been many studies to modify the structure of DTP as well as to lower the HOMO level of the obtained polymer by incorporating the side group into the DTP ring. In 2010, Rasmussen et al. reported N-acyl-substituted DTP-based oligomeric models and introduced carbonyl groups that exhibited the lowered HOMO level, resulting in the devices acquired high V_{OC} of solar cells [13–15]. Hong et al. synthesized the polymer containing N-benzoyl DTP and 4,7-dithieno-2,1,3-benzothiadiazole which gave the PCE of solar cells is 3.95% ($E_g = 1.44$ eV; $J_{SC} = 17.1$ mA/cm^{-2}; $V_{OC} = 0.52$ V) [16]. In 2020, our research reported two D-A conjugated polymers PDTPDPP and PDTPBT based on N-phenyl DTP, DPP and BT with the PCE up to 4.85% ($E_g = 1.31$ eV; $J_{SC} = 12.82$ mA/cm^{-2}; $V_{OC} = 0.79$ V) and 3.99% ($E_g = 1.55$ eV; $J_{SC} = 13.24$ mA/cm^{-2}; $V_{OC} = 0.79$ V), respectively [17].

To design the alternating D-A conjugated polymers, the selection of acceptor units also plays a vital role in reducing polymer bandgap, which is expected to enhance the PCEs. Thieno[3,4-c]pyrrole-4,6-dione (TPD) and benzo[1,2-b:4,5-b']dithiophene (BDT) are known as potential acceptor units due to their planar structures and capability of the formation of quinoidal structures in the excited states [18–21]. In the case of TPD, its quinoidal structure lowers the HOMO energy level of the polymer and makes a high open-circuit voltage (Voc) [18]. In addition, the simple symmetric coplanar structure of TPD can improve the interchain π – π stacking, leading to a higher charge carrier mobility and efficient charge transport in the formed materials [18–24]. In addition, BDT has attracted increasing interest because of its planar structure as well as excellent photovoltaic performance in organic solar cells [5, 25–30]. Interestingly, its two-dimensional (2D) side chains are considered the effective strategy to adjust the energy levels and absorption spectra of obtained polymers. Recently, the conjugated polymer PBDTBTs-BDD have been researched by Hua Tan et al. gave the high PCE of 12.07% ($E_g = 1.8$ eV; $J_{SC} = 23.00$ mA/cm^{-2}; $V_{OC} = 0.79$ V) [31]. These results reveal that TPD and BDT are very promising acceptor/donor moieties for organic solar cells.

In this study, we research the synthesis and characterization of alternating conjugated copolymers in term of donor–acceptor and donor-donor containing *N*-phenyl DTP, TPD and BDT moieties via direct heteroarylation polymerization (DHAP) where the $Pd(OAc)_2$ and $PCy_3.HBF_4$ are used as the catalyst system. The chemical structure and polymer composition of the obtained copolymers was determined by Fourier-transform infrared (FT-IR), gel permeation chromatography (GPC), nuclear magnetic resonance (^{1}H NMR) and X-ray diffraction (XRD) spectroscopies. In addition, the optical properties of copolymers were investigated via Ultraviolet–visible (UV–vis) and Photoluminescence (PL) spectroscopies, while the thermal properties were characterized via differential scanning calorimetry (DSC) and thermogravimetric analysis (TGA). The electrochemical properties of conjugated polymers were investigated by cyclic voltammetry (CV) technique to determine the HOMO – LUMO energy levels. The organic solar cells were fabricated based on these conjugated copolymers with the acceptor unit of $PC_{61}BM$ in the bulk heterojunction construction. The current density–voltage (*J–V*) curves have been recorded to evaluate the PCEs of organic solar cells under the solar simulation of 1.5 AM illumination with an intensity of 100 mW.cm^{-2}. It should be noted that the conjugated polymers based on *N*-phenyl DTP, TPD and BDT moieties have been synthesized and applied for organic solar cells for the first time. In addition, the PCE of donor – acceptor (D-A) and donor – donor (D-D) conjugated polymers based on *N*-phenyl DTP as new donor units have been evaluated in combination with well-known the acceptor and donor units of TPD and BDT, respectively.

Experimental section

Materials

4-hexylaniline was purchased from Biderpharm. 1,1'-Bis(diphenylphosphino)ferrocene (dppf, 98%) were purchased from AK Scientific and used as received. Tricyclohexylphosphine tetrafluoroborate ($PCy_3{\cdot}HBF_4$, 97%), palladium(II) acetate ($Pd(OAc)_2$, 98%), pivalic acid (PivOH, 99%) and 3,3′dibromo-2,2′bithiophene were purchased from Sigma-Aldrich/ Kantochem and used as received. Sodium chloride (NaCl, 99%), potassium carbonate (K_2CO_3, 99%) and sodium *tert*-butoxide (NaO*t*-Bu, 98%) were purchased from Acros/Merck. Tetrahydrofuran (99.9%) and *N*-bromosuccinimide were purchased from Acros Organics. Dimethylacetamide (DMAc, 99%), toluene (99.5%) and chloroform ($CHCl_3$, 99.5%) were purchased from Fisher/Acros and dried using molecular sieves under N_2. Methanol (99.8%), dichloromethane (99.8%), *n*-hexane (99%), and ethyl acetate (99%) were purchased from Fisher/Acros and used as received.

Measurements

^{1}H NMR spectra were recorded in deuterated chloroform ($CDCl_3$) with tetramethylsilane (TMS) as an internal reference, on a Bruker Avance 500 MHz. Fourier transform infrared (FT-IR) spectra, collected as the average of 264 scans with a resolution of 4 cm^{-1}, were recorded from a KBr disk on the FT-IR Bruker Tensor 27. Size exclusion chromatography (SEC) measurements were performed on a Polymer PL-GPC 50 gel permeation chromatography system equipped with an RI detector, with tetrahydrofuran as the

eluent at a flow rate of 1.0 mL/min at room temperature. The column of PL-GPC 50 gel permeation chromatography is polystyrene and molecular weight and molecular weight distribution were calculated with reference to polystyrene standards. Elemental analyses were performed by the Dumas combustion method, using a Costech ECS 4010 Elemental Analyzer.

UV–vis absorption spectra of polymers in solution and polymer thin films were recorded on an Agilent 8453 spectrometer over a wavelength range of 200–900 nm. Fluorescence spectra were measured on an Ocean Optics SF-2000 and Varian Cary Eclipse fluorescence Spectrometer with the slits widths of 5 nm.

Differential scanning calorimetry (DSC) measurements were carried out with TA instruments TA2910 under nitrogen flow (heating rate 10 °C min^{-1}). Thermogravimetric analysis (TGA) measurements were performed under nitrogen flow using TA2950 Instruments with a heating rate of 10 °C min^{-1} from ambient temperature to 1000 °C. Wide-angle powder XRD patterns were recorded at room temperature on a Bruker AXS D8 Advance diffractometer using Cu-K_α radiation (k = 0.15406 nm), at a scanning rate of 0.05°s^{-1}. The data were analyzed using DIFRAC plus Evaluation Package (EVA) software. The *d*-spacing was calculated from peak positions using Cu-K_α radiation and Bragg's law. Atomic force microscopy (AFM) images were obtained using a Bruker Dimension 3100 atomic force microscope.

Electrochemical measurements were performed on an AUTOLAB machine (software NOVA 1.11) using an Au disc working electrode and a Pt wire counter electrode. Solutions consisted of 0.1 M TBAPF6 in CH_3CN and were sparged with argon for 20 min prior to data collection. All potentials are referenced to a Ag/Ag + reference electrode (0.1 M $AgNO_3$/0.1 M TBAPF6 in CH_3CN; 0.320 V vs. SCE) and internally standardized with ferrocene (vs. Ag/Ag +). E_{HOMO} values were determined in reference to ferrocene. The polymer film was coated on an electrode washed with CH_3CN and placed in a cell with a fresh electrolyte solution for electrochemical characterization.

Synthesis of 4-(4-hexylphenyl)-4H-dithieno[3,2-b:2', 3'd]pyrrole (HPDTP) (monomer 1)

To a 100 mL two-necked round bottom flask was added 3,3'-dibromo-2,2'-bithiophene (1000 mg, 3.09 mmol), 4-hexylaniline (712 mg, 4.01 mmol), $Pd_2(dba)_3$ (29 mg, 0.03 mmol), dppf (69 mg, 0.12 mmol) and sodium tert-butoxide (1187 mg, 12.34 mmol). The mixture was dissolved in dry toluene under nitrogen and degassed via freeze–pump–thaw cycle for three times. After that, the reaction mixture was heated at 110 °C for 24 h, then allowed to cool to room temperature and 50 mL of dichloromethane was added. The organic layer was dried over anhydrous K_2CO_3 and solvent was removed by evaporation. The crude product was purified over SiO_2 using dichloromethane/*n*-hexane (1:10, v/v) to obtain a pure compound as a deep brown solid (1048 mg, 91%).

^{1}H NMR (500 MHz, $CHCl_3$), δ (ppm): 7.47 (d, J = 8.4 Hz, 2H), 7.32 (d, J = 8.4 Hz, 2H), 7.15 (q, J = 5.2 Hz, 4H), 2.67 (t, J = 7.2 Hz, 2H), 1.67 (m, 2H), 1.35 (m, 6H), 0.91 (t, J = 6.4 Hz, 3H). Elemental Analysis for $C_{10}H_{21}NS_2$: calculated C, 70.75; H, 6.23; N, 4.13; S, 18.89. Found: C, 71.12; H, 6.09; N, 4.27; S,18.52.

Synthesis of 1,3-dibromo-5-(2-ethylhexyl)-4H-thieno[3,4-c]pyrrole-4,6(5H)-dione (DBTPD) (monomer 2)

To a solution of 300 mg (1.26 mmol) 5-(2-ethylhexyl)-4H-thieno[3,4-c]pyrrole-4,6(5H)-dione in a mixture of sulfuric acid (1.80 mL) and trifluoroacetic acid (3.90 mL). Then, 604 mg (2.53 mmol) of *N*-bromosuccinimide was added slowly into the flask under an ice-water bath. Then, the reaction mixture was stirred at room temperature for 24 h. After completion of the reaction, the reddish-brown compound was extracted with 50 mL of dichloromethane, washed with distilled water for three times. The organic layer was dried over anhydrous K_2CO_3 followed by concentrating under reduced pressure. The crude product was purified by silica gel column chromatography using chloroform/*n*-hexane (2:3, v/v) as eluent to afford the white crystalline solid product, 288 mg, 58% yield.

^{1}H NMR (500 MHz, $CHCl_3$), δ (ppm): 3.49 (2H, d, J = 6.4 Hz), 1.78 (1H, m), 1.30 (8H, m), 0.91 (6H, m, J = 7.6 Hz). Elemental Analysis for $C_{14}H_{17}Br_2NO_2S$: calculated C, 39.74; H, 4.05; Br, 37.77; N, 3.31; O, 7.56; S, 7.58; Found: C, 39.96; H, 3.93; Br, 36.54; N, 3.42; O, 8.37; S, 7.78.

Synthesis of 2,6-dibromo-4,8-bis(hexyloxy) benzo[1,2-b:4,5-b']dithiophene (DBBDT) (monomer 3)

4,8-bis(hexyloxy)benzo[1,2-b:4,5-b']dithiophene (400 mg, 1.02 mmol) was dissolved into 10 mL of dichloromethane in a 100 mL flask under nitrogen. Then, NBS (365 mg, 20 mmol) was dissolved into 10 mL of dichloromethane in a funnel and slowly dropped into the flask under an ice-water bath, and then the reactant was stirred for 24 h at ambient temperature. After that, the reactant was extracted by chloroform, washed with NaCl solution and distilled water for several times. The mixture evaporated to obtain the crude product which was purified by silica gel chromatography with *n*-hexane as eluent. A yield of 144 g of 2,6-dibromo-4,8-bis(hexyloxy)benzo[1,2-b:4,5-b']dithiophene (yield 26%) was obtained as a pale yellow solid.

^{1}H NMR (500 MHz, $CHCl_3$), δ (ppm): 7.41 (s, 2H), 4.19 (t, 4H), 1.83 (m, 4H), 1.53 (m, 4H), 1.36 (m, 8H), 0.93 (m,

6H). Elemental Analysis for $C_{22}H_{28}Br_2O_2S_2$: calculated C, 48.18; H, 5.15; Br, 29.14; O, 5.83; S, 11.69; Found: C, 47.88; H, 5.47; Br, 28.06; O, 6.24; S, 12.35.

Synthesis of donor–acceptor poly(4-(4-hexylphenyl)-4H-dithieno[3,2-b:2',3'-d]pyrrole-alt-5-(2-ethylhexyl) -4H-thieno[3,4-c]pyrrole-4,6(5H)-dione) (Poly(HPDTP-alt-TPD)) (P1)

HPDTP (100 mg, 0.29 mmol) and DBTPD(125 mg, 0.29 mg) were dissolved in 10 mL of DMAc in a 100 mL flask under nitrogen. Then, $Pd(OAc)_2$ (3.40 mg, 0.01 mmol), $PCy_3.HBF_4$ (10.90 mg, 0.03 mmol), PivOH (30.10 mg, 0.29 mmol) and K_2CO_3 (123 mg, 0.88 mmol) were added into the flask. Next, the solution was degassed via freeze–pump–thaw cycle three times followed by heating at 110 °C and stirring for 24 h. After that, the mixture was cooled down to room temperature, and the polymer was precipitated by dropping slowly into the flask of 50 mL of methanol under an ice-water bath and filtered through a Soxhlet system with methanol, *n*-hexane, and chloroform. The resulting solution from the chloroform fraction was precipitated once more by the addition of 50 mL of methanol and then isolated by filtration. The polymer was recovered as a dark brown solid which was dried under vacuum at 50 °C for 24 h to obtain conjugated polymer P1 (78.5 mg, yield 66%).

^{1}H NMR (500 MHz, $CDCl_3$), δ (ppm): 8.1 (s, 1H), 7.48 (d, 2H), 7.37 (d, 2H), 7.09 (s, 1H), 3.53 (m, 2H), 2.70 (s, 2H), 1.86 (s, 1H), 1.70 (m, 4H), 1.36 (m, 12H), 0.92 (m, 9H). GPC: $M_n = 8900$ g/mol. Đ (M_w/M_n) = 1.36.

Synthesis of donor-donor Poly(4-(4-hexylphenyl)-4H-dithieno[3,2-b:2',3'-d]pyrrole-alt-4,8-bis(hexyloxy)benzo[1,2-b:4,5-b']dithiophene) (Poly(HPDTP-alt-BDT)) (P2)

HPDTP (100 mg, 0.29 mmol) and DBBDT(162 mg, 0.29 mg) were dissolved in 10 mL of DMAc in a 100 mL flask under nitrogen. Then, $Pd(OAc)_2$ (3.40 mg, 0.01 mmol), $PCy_3.HBF_4$ (10.90 mg, 0.03 mmol), PivOH (30.10 mg, 0.29 mmol) and K_2CO_3 (123 mg, 0.88 mmol) were added into the flask. Next, the solution was degassed via freeze–pump–thaw cycle three times followed by heating at 110 °C and stirring for 24 h. After that, the mixture was cooled down to room temperature, and the polymer was precipitated by dropping slowly into the flask of 50 mL of methanol under an ice-water bath and filtered through a Soxhlet system with methanol, *n*-hexane, and chloroform. The resulting solution from the chloroform fraction was precipitated once more by the addition of 50 mL of methanol and then isolated by filtration. The polymer was recovered which was dried under vacuum at 50 °C for 24 h to give 192.6 mg of the final product as a deep reddish-brown solid (76% yield).

^{1}H NMR (500 MHz, $CDCl_3$), δ (ppm): 7.25–7.75 (m, 4H), 6.5–7.25 (m, 4H), 4.25 (m, 4H), 2.71 (m, 2H), 0.96–1.89 (m, 35H). GPC: $M_n = 8700$ g/mol. Đ (M_w/M_n) = 1.44.

Fabrication of bulk-heterojunction organic solar cells

In the beginning, The ITO substrates (10Ω/sq) were cleaned via ultrasonication with deionized water, acetone and isopropyl alcohol respectively. The device configuration of organic solar cells was fabricated with a bulk heterojunction (BHJ) structure of ITO/PEDOT:PSS/conjugated polymers:$PC_{61}BM$/Al. First, the PEDOT:PSS layer was coated on ITO by spin coating machine, the dried under oven 100° C for 15 min and transferred into a N_2 glowbox to spin coating the activate layer of conjugated polymer:$PC_{61}BM$ (weight ratio 1:1.15) in chlorobenzene solvent with 1.0 vol% of 1,8-diiodooctane (DIO). The activated films of conjugated polymer:$PC_{61}BM$ were treated by thermal annealing at 100° C for 10 min. Finally, the electrode of Al was deposited by thermal evaporation in a vacuum of 10^{-7} torr via the diffusion pump system. The obtained organic solar cells were recorded to assess the PCE via current density–voltage (*J–V*) curves using Keithley 2400 source meter under ABET solar simulator of AM 1.5G.

Results and discussion

Synthesis and characterization of D-A and D-D conjugated polymers P1 and P2

The synthetic route for preparation of monomers including 4-(4-hexylphenyl)-4H-dithieno[3,2-b:2',3'd]pyrrole (HPDTP) (1), 1,3-dibromo-5-(2-ethylhexyl)-4H-thieno[3,4-c]pyrrole-4,6(5H)-dione (DBTPD) (2) and 2,6-dibromo-4,8-bis(hexyloxy)benzo[1,2-b:4,5-b']dithiophene (DBBDT) (3) is presented in Scheme S1 (see supporting information, Scheme S1). HPDTP (monomer 1) was synthesized by nucleophilic substitution of 4-hexylaniline with 3,3′-dibromo-2,2′-bithiophene with the yield reaction of 91%. The TPD monomer has been synthesized from thiophene-3,4-dicarboxylic acid and acetic anhydride to obtain thieno[3,4-c]furan-1,3-dione which reacted with 2-ethyl-1-hexylamine, then $SOCl_2$ to form 4-(octylcarbamoyl)thiophene-3-carboxylic acid (TPD) in the yield of 65% [32, 33]. Then, TPD was brominated to form 1,3-dibromo-5-(2-ethylhexyl)-4H-thieno[3,4-c]pyrrole-4,6(5H)-dione (DBTPD) (monomer 2). The 2,6-dibromo-4,8-bis(hexyloxy)benzo[1,2-b:4,5-b']dithiophene (DBBDT) (monomer 3) was obtained via the bromination reaction of commercial 4,8-bis(hexyloxy)benzo[1,2-b:4,5-b']dithiophene. All synthesized monomers were analyzed by ^{1} H NMR and exhibited all characteristic peaks which are reasonable with their chemical structures (see SI, Figs. S1–S3).

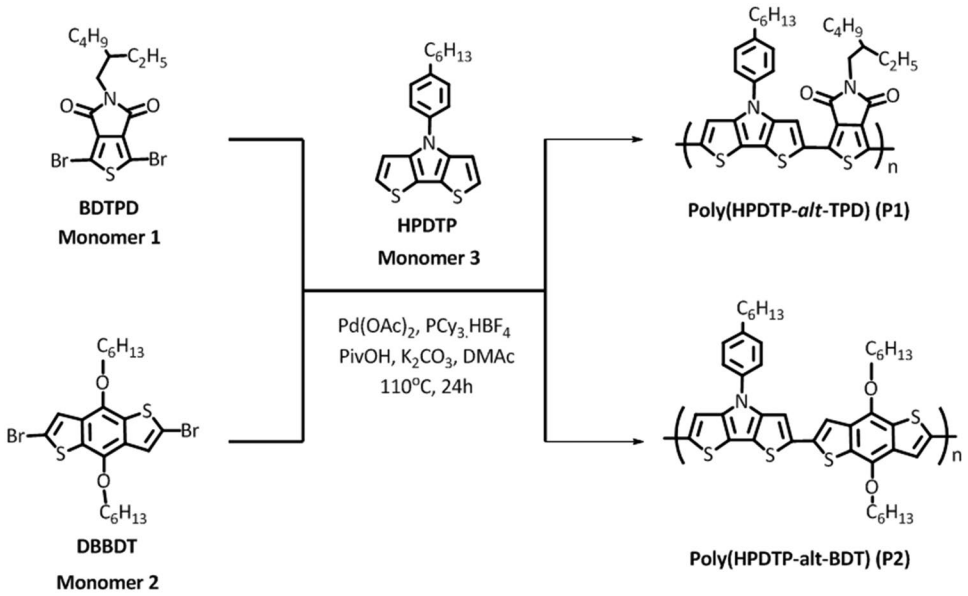

Scheme 1 Synthesis of D-A and D-D conjugated polymers P1 and P2

Following, the monomer 1, monomer 2 and monomer 3 were used to polymerized the corresponding conjugated polymers via direct arylation polymerization that performed in DMAc solvent at 110° C with $Pd(OAc)_2$ as the catalyst and $PCy_3.HBF_4$ as the ligand. The synthesis and reaction conditions of conjugated polymers P1 and P2 were presented in Scheme 1. At the beginning of the reactions, the colors of reactions were light yellow, then they changed to orange in the case of P1 and deep red in the case of P2 after 24 h. The obtained conjugated polymers were filtrated through a Celite layer to remove the Pd catalyst followed by precipitation by methanol. Continuously, the conjugated polymers were treated by Soxhlet with heptane, dichloromethane and chloroform respectively. The yields of polymerizations were calculated by the mass of polymers in $CHCl_3$ fraction which showed the yield of polymers P1 and P2 were about 66% and 76%, respectively. Both conjugated polymers also exhibited good solubility in common solvents such as THF, chloroform and chlorobenzene. The average molecular weight of conjugated polymers (M_n) was evaluated by a gel permeation chromatography (GPC) which showed the M_n of P1 and P2 are 8900 g/mol and 8700 g/mol with polydispersity indexes (Đ) of 1.36 and 1.44, respectively (Fig. 1). The GPC curves of polymers exhibited the symmetrical shape that indicated that the polymer chains are relatively homogeneous.

The FTIR spectra of the alternating conjugated polymers P1 and P2 showed all characteristic bands (see SI, Fig. S4). The multipeaks from 2859 cm^{-1} and 3097 cm^{-1} attributed to C-H stretching of the *n*-hexyl group and ring C-H stretching vibrations. The peaks at 1.522 cm^{-1} and 1.392 cm^{-1} are ascribed to the aromatic C=C stretching and C-N stretching of pyrrole moieties, respectively [34]. In addition, the characteristic peak at 1694 cm^{-1} is assigned for C=O stretching vibration of polymer P1 and the peak at 1038 cm^{-1} indicates the presence of phenyl C-O group of BDT moieties in P2. Moreover, the peaks, which appeared at around 638 cm^{-1}, corresponded to the S–C stretching vibrations.

The ^{1}H NMR spectroscopy has been used to determine the structure of the conjugated polymers P1 and P2. In the ^{1} H NMR spectrum of P1 (Fig. 2A), the peaks from 0.92 ppm to 2.70 ppm are attributed to the alkyl side chains of polymer P1. The peak at 3.53 ppm (peak "I") that is assigned to the methylene protons next to nitrogen atom in 4H-thieno[3,4-c]pyrrole-4,6(5H)-dione moieties. In addition, the peaks from 7.09 ppm to 8.10 ppm (peak "a", "b", "c" and "d") which corresponds to the aromatic protons in 4-(4-hexylphenyl)-4H-dithieno[3,2-b:2',3'-d] pyrrole and 5-(2-ethyl hexyl) -4H-thieno[3,4-c]pyrrole-4,6(5H)-dione units. It should be noted that the integration of peak "e" which is attributed to the methylene protons of 4-(4-hexylphenyl)-4H-dithieno[3,2-b:2',3'-d]pyrrole is equal to the integration of peak "i" of methylene protons of 5-(2-ethyl hexyl) -4H-thieno[3,4-c]pyrrole-4,6(5H)-dione, this result indicated that the composition of building donor and acceptor units in alternating D-A conjugated polymers P1 is 1:1. This results also confirmed that direct (hetero) arylation polymerization was successfully performed to form the desired conjugated polymer P1. In the case of polymer P2, the ^{1}H NMR spectrum showed in Fig. 2B, the peaks from 0.96 ppm to 2.71 ppm are also corresponding to the alkyl side chains of polymer P2. The peak at 4.25 ppm (peak "h") attributed to the methylene protons which is adjacent to the oxygen atom of 4,8-bis(hexyl oxy)benzo[1,2-b:4,5-b']dithiophene) moieties. The broad peaks from 6.90 ppm to 7.5 ppm are assigned to aromatic proton of both building thiophenes units. In addition, the integration of peak

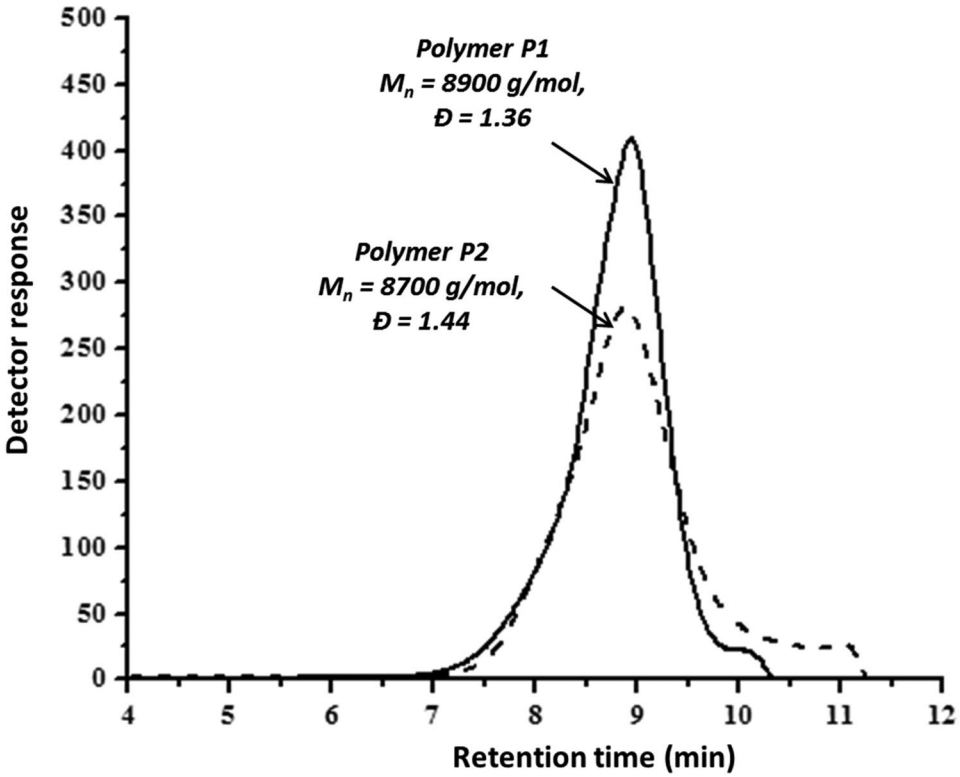

Fig. 1 GPC curves of the alternating conjugated polymers P1 and P2

"g" that is attributed to methylene protons in side chains of 4-(4-hexylphenyl)-4H-dithieno[3,2-b:2',3'd]pyrrole has a haft of the integration of peak "h" which are also assigned to methylene protons of 4,8-bis(hexyl oxy)benzo[1,2-b:4,5-b']dithiophene), this result determined that the composition of donor and acceptor units in alternating D-A conjugated polymer P2 is 1:1.

Optical and thermal properties of D-A conjugated polymers

The conjugated polymer P1 (M_n: 8900 g/mol, Đ: 1.36) and P2 (M_n: 8700 g/mol, Đ: 1.44) were dissolved in THF solvent with concentration of ca. 10^{-6} mol.L^{-1} and were prepared with a thin film on quartz substrate to determine the absorption properties of polymers (Fig. 3A). The conjugated polymer P1 exhibited an absorption maximum at 540 nm in THF, whereas the polymer P2 showed a slightly red-shifted absorption at 550 nm. The conjugate polymer films were prepared via spin coating on quartz substrate and annealed at 150 °C in 10 min for UV – Vis characterization of solid state film. Both conjugated polymers film of P1 and P2 exhibited the maximal absorption at 510 nm as shown in Fig. 3B. In addition, the solid state film of the conjugated polymer P1 and P2 film which prepared by non- annealed exhibited the maximal absorption at 565 nm and 575 nm, respectively (Fig. S7). These results suggested that the annealing process at 150 °C caused the degradation of small segments in conjugated polymers.The polymer P1 exhibited an onset absorption located at 690 nm which is corresponding to an optical bandgap (E_g^{opt}) of 1.80 eV, while the polymer P2 showed the onset absorption at 640 nm attributed to an optical bandgap of 1.94 eV. It is recognized that polymer P1 which contains the hard TDP moieties has a red-shifted absorption caused by the stronger intermolecular interactions. The molar extinction coefficient (ε) of polymers P1 and P2 were calculated about 0.95×10^6 and 1.02×10^6 (mol^{-1} L cm^{-1}), respectively.

The photoluminescent spectra (PL) of conjugated polymers P1 and P2 were performed in different solvents with concentration of ca. 10^{-3} mol.L^{-1} to investigate the emission wavelength of polymers under a wavelength excitation at 540 nm. The polymer P1 exhibited emission peaks of 570 nm in $CHCl_3$ and 600 nm in THF (Fig. 4A). Meanwhile, the polymer P2 showed emission peaks at 608 nm and 610 nm for $CHCl_3$ and THF, respectively (Fig. 4B). The fluorescence quantum yields (ΦF) of these conjugated polymers in dilute $CHCl_3$ were analyzed in comparison to 9,10-diphenylanthracene as a standard (ΦF = 0.9). The ΦF of P1 and P2 have the value of 0.53 indicating the strong π –π stacking effect in both polymer structures [35]. The UV – Vis and PL data are summarized in Table 1.

Thermal properties of obtained conjugated polymers were characterized by thermogravimetric analysis (TGA) and differential scanning calorimetry (DSC) to consider the thermal stability of polymers. The TGA curves showed the good thermal stability of polymers with 5% weight loss

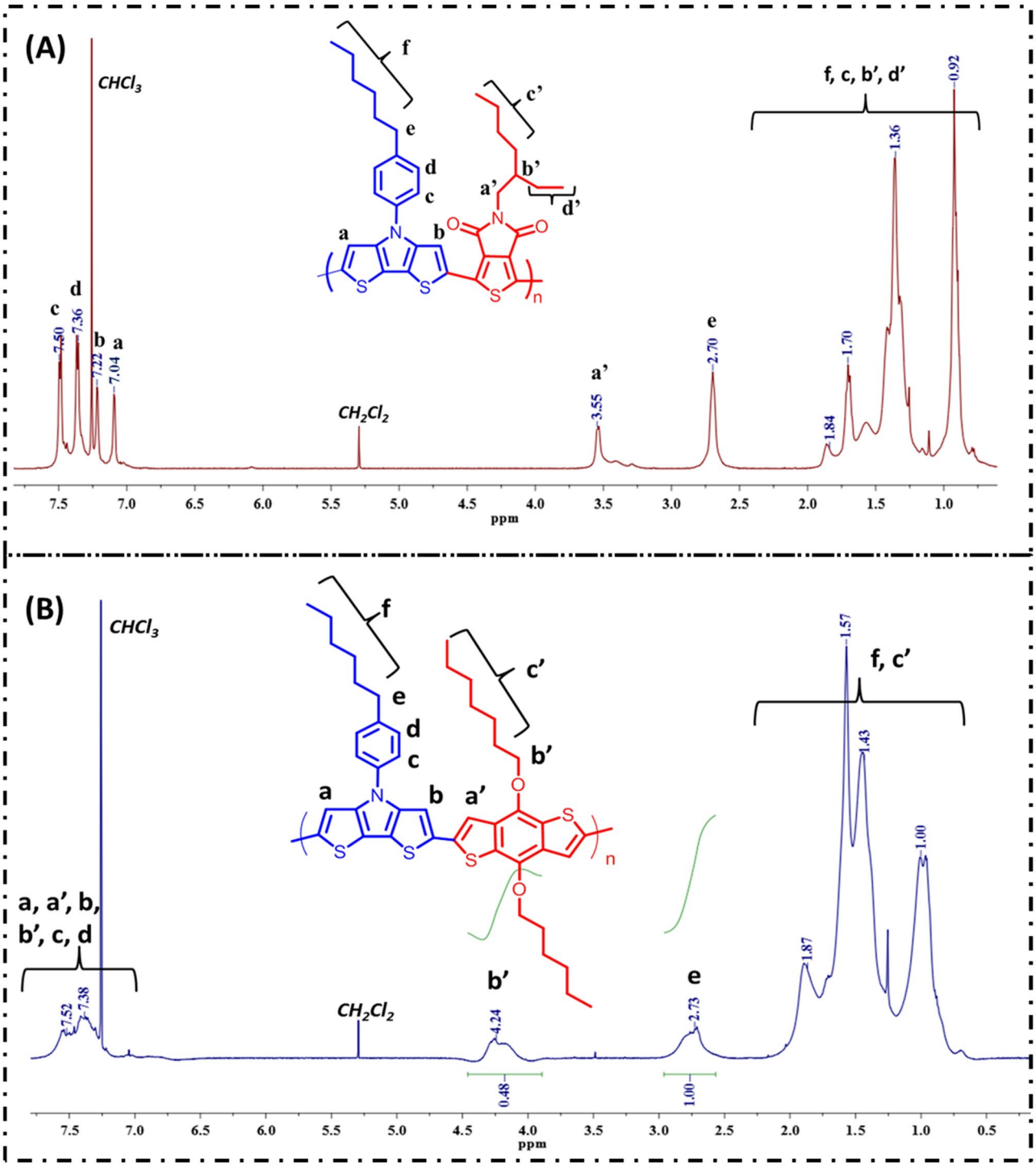

Fig. 2 ^{1}H NMR spectra of the alternating conjugated polymers P1 (**A**) and P2 (**B**)

temperatures (T_d) at 400 °C and 350 °C for polymer P1 and P2, respectively (Fig. 5A). The first heating running DSC were performed from room temperature to 150 °C to remove the moieties as well as a impurities small molecules. Then, the second heating running DSC curves were performed from room temperature to 300 °C for polymers P1 and P2 are showed in Fig. 5B. It is clearly that no melting point of polymers was observed in this temperature range. Normally, the backbone of conjugated polymers is very stiff and conjugated polymer chains have a strong π –π stacking intermolecular that lead to the almost conjugated polymer structures are thermal stability and high melting point. However, there is a

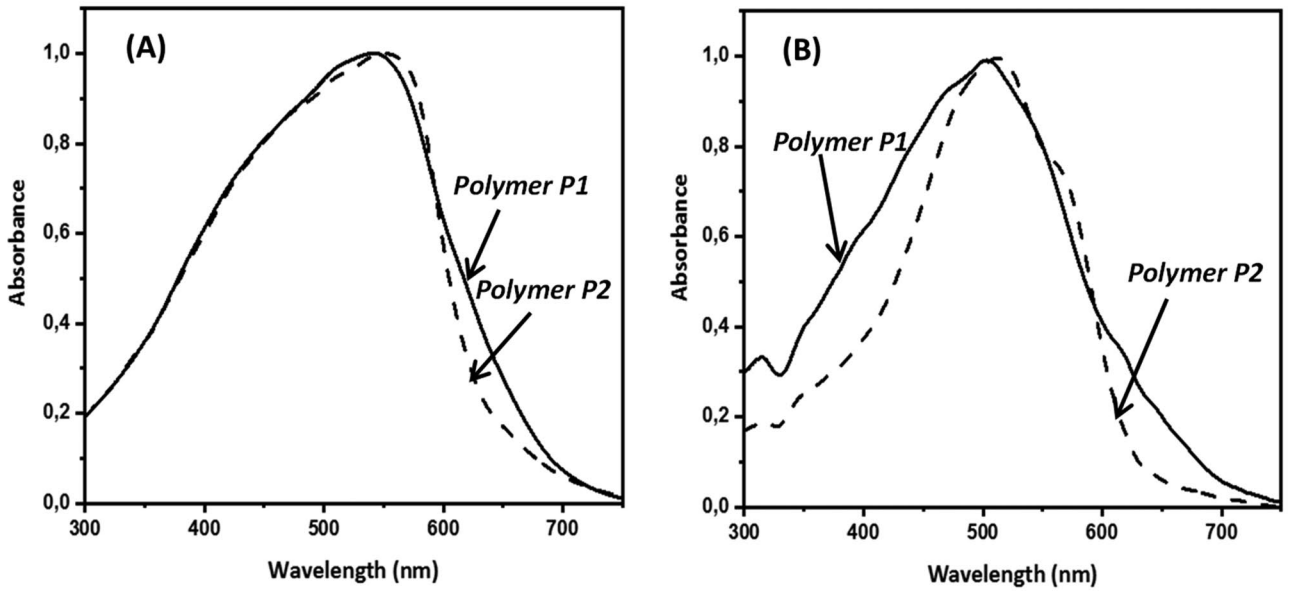

Fig. 3 The UV–Vis spectra of conjugated polymers P1 and P2 in solution (**A**) and in thin film (**B**)

glass transition temperature at 180 °C for conjugated polymers P1 which is attributed for a glass transition temperature of hexyl side chains of polymers. On the contrary, there is not a glass transition temperature observed for polymer P2.

Electrochemical properties of D-A conjugated polymers

Cyclic voltammetry (CV) measurement was carried out to investigate the redox properties of D-A conjugated polymers. The polymers were dissolved in chlorobenzene (CB) and coated on the platinum working electrode to form the thin films for CV studies. The obtained CV curves were referenced to an Ag/Ag+ electrode, which were calibrated using the ferrocene/ferrocenium redox couple as an internal standard [36]. The HOMO (the highest occupied molecular orbital) levels of polymers P1 and P2 were estimated from the onset potential of the first oxidation wave which related to the energy levels of ferrocene reference (4.8 eV below the vacuum level). On the

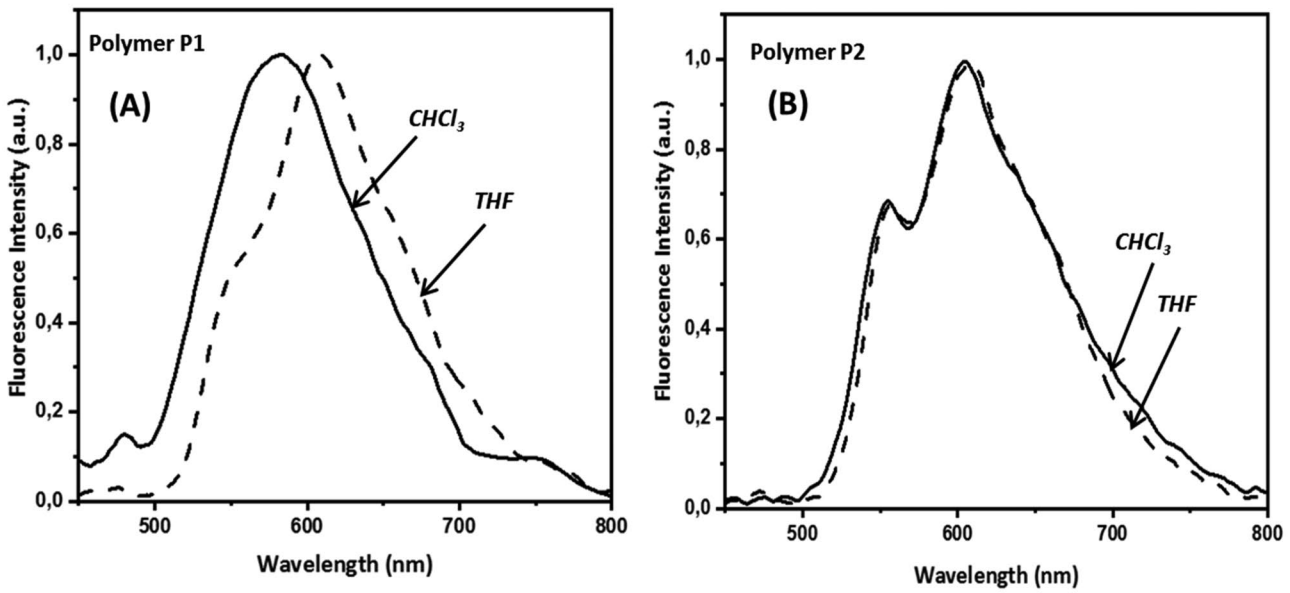

Fig. 4 PL spectra of conjugated polymers P1 (**A**) and P2 (**B**) in $CHCl_3$ and in THF solvent

Table 1 Optical properties of D-A conjugated polymers P1 and P2

Entry	Conjugated Polymers	UV (λ_{max}) (nm)		PL (nm)		φ_F	Optical bandgap (E_g^{opt}) (eV)	Molar extinction coefficient (ε)
		Solution	Film	$CHCl_3$	THF			
1	P1	540	503	570	598	0.53	1.80	0.95×10^6
2	P2	550	512	608	610	0.53	1.94	1.02×10^6

other hand, the LUMO (the lowest unoccupied molecular orbital) levels were calculated by the onset of absorption spectra. The CV curves and energy levels diagram are displayed in Fig. 6. The CV diagram showed an oxidation onset potential of conjugated polymer P1 at 0.62 V attributed to the HOMO energy level of –5.02 eV. In the case of polymer P2, the CV measurement exhibited an oxidation onset potential at 0.78 eV corresponding to the HOMO energy level of –5.18 eV. The LUMO energy levels of polymer P1 and P2 were determined based on HOMO level and optical band gaps to be –3.22 eV and –3.24 eV for P1 and P2, respectively. The LUMO levels of these polymers were close to the LUMO of the PCBM acceptor, which indicated that the polymers P1 and P2 were potential materials for organic solar cells. The HOMO and LUMO levels as well as the estimated band gaps of the conjugated polymer P1 and P2 were presented in Table 2.

The conjugated polymer P1 and P2 in the solid state were characterized via X-ray diffraction (XRD) measurements. The XRD pattern of polymer P1 and P2 reveal only a broad amorphous diffraction located at $2\theta = 22.0°$ (Fig. S6). The conjugated polymers were exhibited the as small fibres via TEM morphologies at the scale of 200 nm (Fig. S5). The thin film of D-A conjugated polymer P1 and P2 helped investigate the microscopic and nanoscopic morphologies via AFM tapping contact mode. The polymer thin films were spin coated onto wafer substrate from chlorobenzene, then annealed at 150 °C for 15 min. As shown in Fig. 7, the thin film of polymer P2 exhibited the AFM surface is smoother than of polymer P1. The roughness (RMS) of conjugated polymers P1 and P2 were defined about 11.87 and 1.45 respectively. It is noted that the solubility of P2 in solvents was much better than P1 due to the density of alkoxy side chains, and therefore the results revealed that the surface of P2 was smoother than that of P1.

Organic solar cell based on Bulk heterojunction (BHJ)

The conventional structure of ITO/PEDOT:PSS/Polymer P1/P2:$PC_{61}BM$ (1:1.15)/Al has been used to fabricate the bull heterojunction (BHJ) organic solar cells. The J_{SC}, V_{OC}, fill factor (FF) have been recorded under solar simulation of

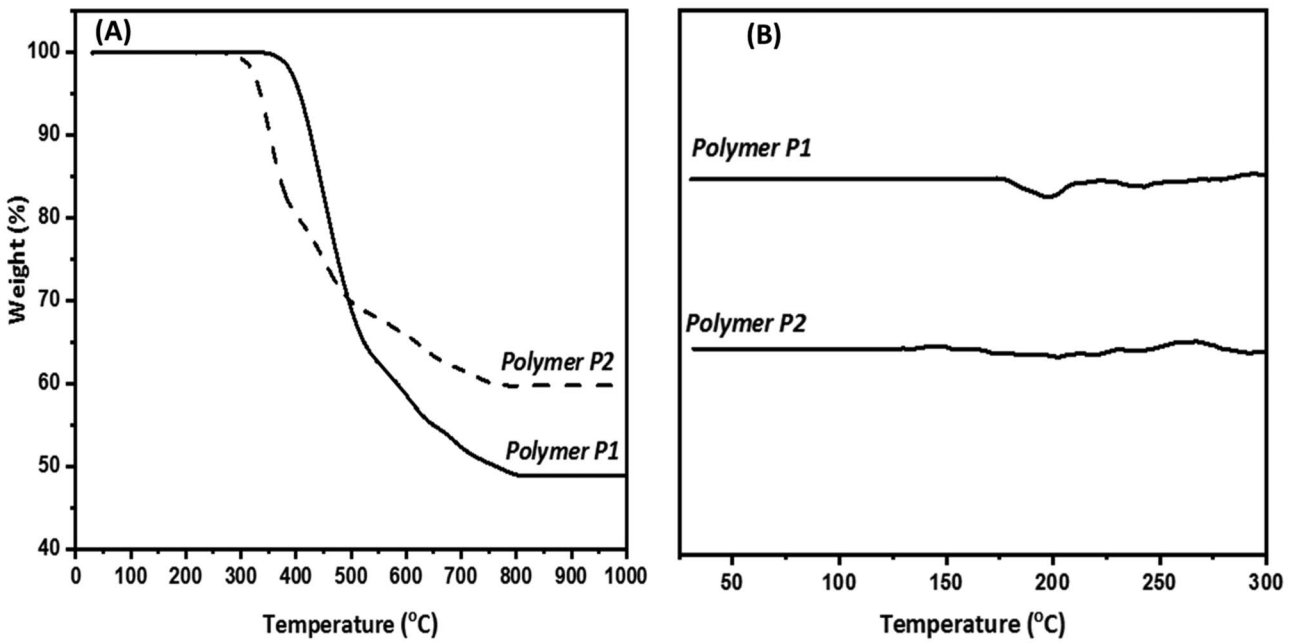

Fig. 5 The TGA (**A**) and DSC (**B**) curves of conjugated polymers P1 and P2

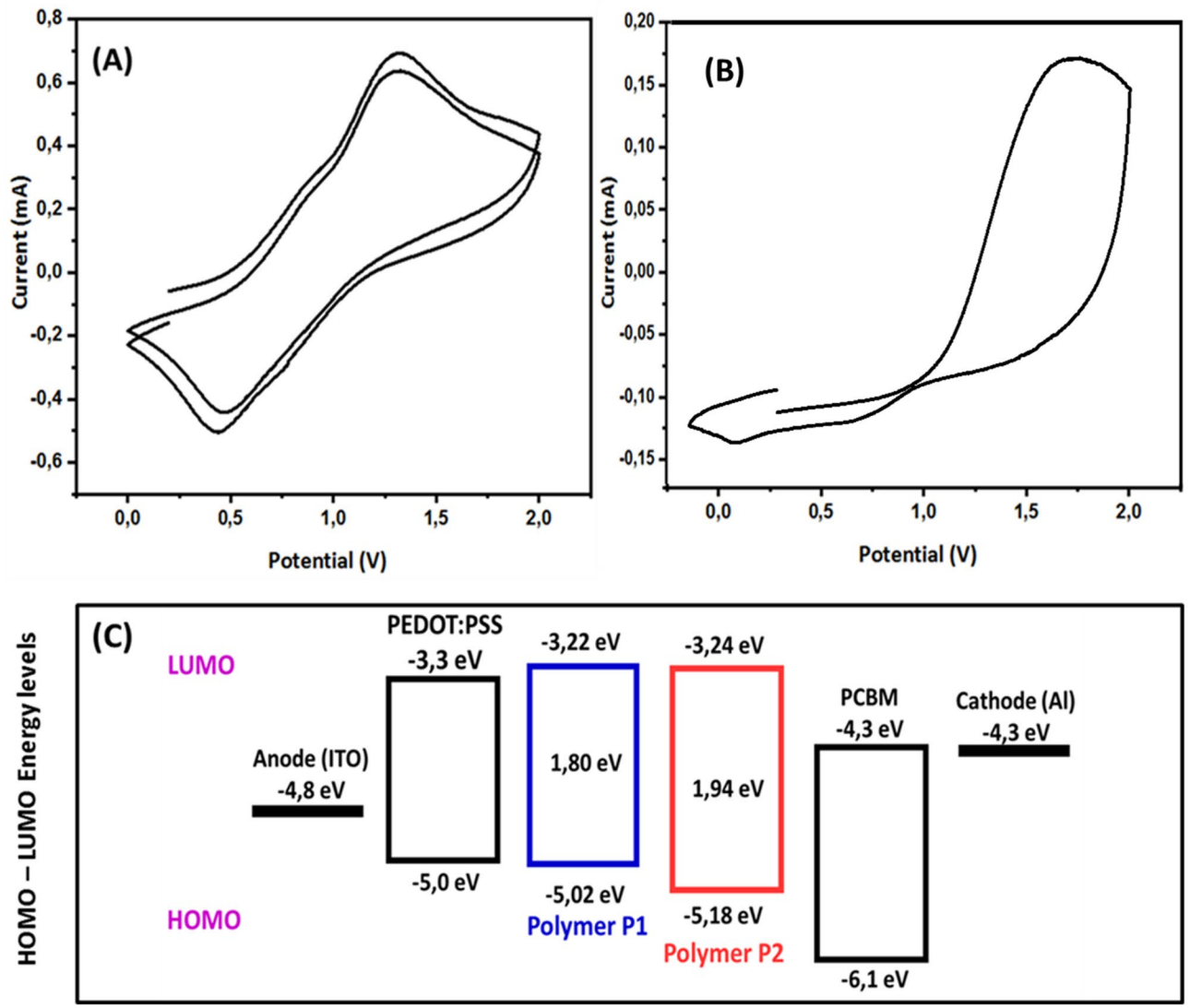

Fig. 6 Cyclic Voltammetry curves of polymers P1 (**A**) and P2 (**B**) and the illustration of HOMO – LUMO energy levels of polymers (**C**)

1.5G via I-V characterization (Keithley 2400 source meter) (Fig. 8A). The parameter of organic solar cells based on these conjugated polymers is presented in Table 3. The OSCs based on polymer P1 exhibited the V_{OC} of 085 V and J_{SC} of 10.5 mA, which is attributed to the average PCE of 3.65%. Meanwhile, the polymer P2 showed the V_{OC} of 0.78 V and J_{SC} of 10.9 mA, which corresponds to the average PCE of 3.35%. The EQE spectra of organic solar cell devices based on polymer P1 and P2 exhibited a pronounced contribution to photocurrent generation in the wavelength range of 300–850 nm (Fig. 8B). Based on the results of PCEs of organic solar cells fabricated from D-A and D-D conjugated polymers P1 and P2, it is confirmed that the role of acceptor moieties in conjugated polymers which induces the lower bandgap as well as their HOMO – LUMO energy levels is matched with HOMO–LUMO levels of acceptor PCBM and the holes transport layer components.

Table 2 Electrochemical properties of the conjugated polymer P1 and P2

Entry	Polymers	E_{ox}^{onset} (V)[a]	E_g (eV)[b]	HOMO (eV)[c]	LUMO (eV)[d]
1	P1	0.62	1.80	–5.02	–3.22
2	P2	0.78	1.94	–5.18	–3.24

[a]Onset oxidation potential vs Ag/AgCl

[b]Estimated from the onset of absorption edge

[c]Estimated from the onset oxidation potential

[d]Deduced from HOMO and E_g

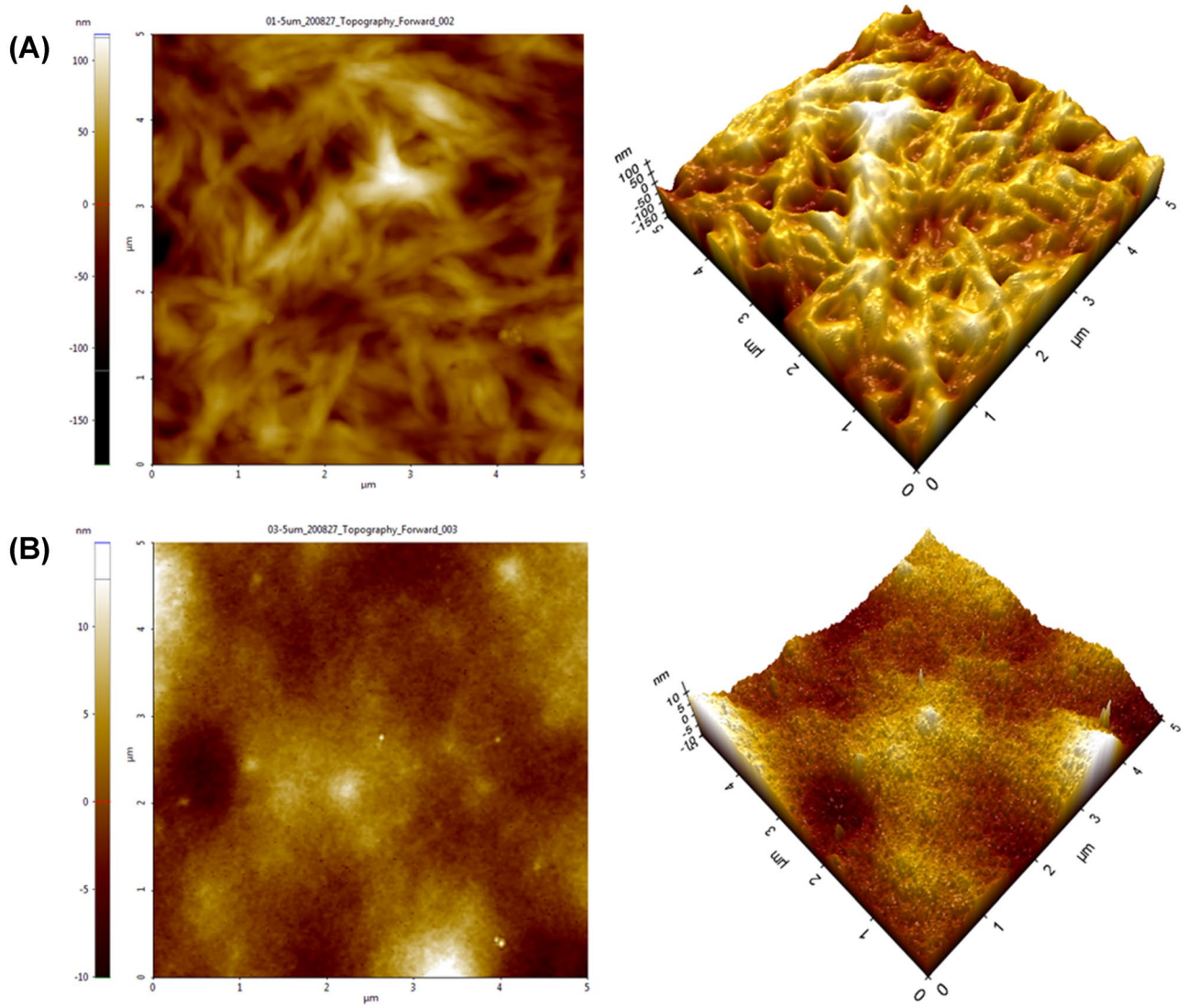

Fig. 7 AFM images of D-A polymer P1 (**A**), and polymer P2 (**B**)

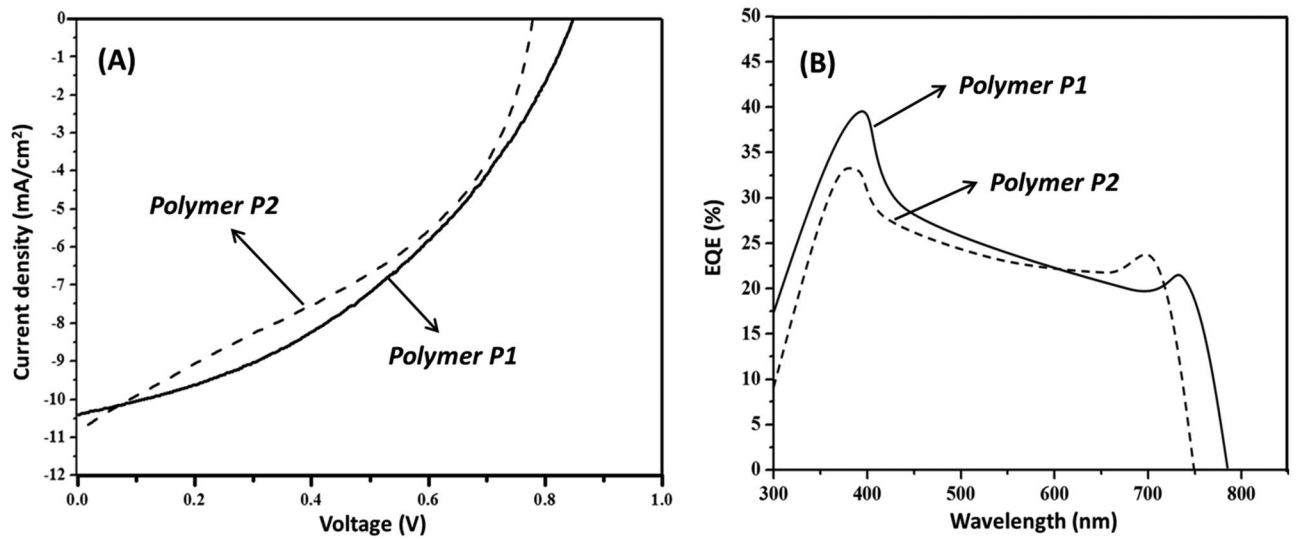

Fig. 8 Current–voltage characteristics of the bulk heterojunction polymeric solar cells based on polymers P1 and P2 (**A**) and EQE spectra of solar cells based on P1 and P2 (**B**)

Table 3 The I-V parameter of organic solar cells fabricated on polymers P1 and polymer P2 using acceptor $PC_{61}BM$ under the illumination of AM 1.5G, 100 mW cm^{-2}

D-A Polymer/Fullerene	V_{oc} (V)	J_{sc} (mA/cm^2)	FF (%)	PCE (Avg.) %
$P_1/PC_{61}BM$	0.85	10.50	40.97	3.65
$P_2/PC_{61}BM$	0.78	10.90	39.46	3.35

Conclusion

In conclusion, novel designed D–A and D-D alternating conjugated polymers containing a dithieno [3,2-b:2',3'-d] pyrrole, thieno[3,4-c]pyrrole-4,6-dione and benzo[1,2-b:4,5-b']dithiophene moieties have been synthesized successfully via direct (hetero) arylation polymerization method. The obtained conjugated polymers of P1 and P2 exhibited the band gaps of 1.80 eV and 1.94 eV, respectively. The HOMO–LUMO energy levels of the resulting conjugated polymers are reasonable for bulk heterojunction organic solar cells based on the $PC_{61}BM$ acceptor counterpart. The organic solar cells based on D-A and D-D conjugated polymer P1 and P2 have been fabricated and recorded the average PCE of 3.65% and 3.35%, respectively. These conjugated polymers P1 and P2 would be useful to fabricate the organic solar cells in the modern term of all conjugated polymers.

Supplementary information The online version contains supplementary material available at https://doi.org/10.1007/s10965-022-02969-9.

Acknowledgements This research was fully supported by the Vietnam National Foundation for Science and Technology Development (NAFOSTED) under grant number ''104.02-2020.39"

Declarations

Conflict of interest All authors declare that they have no conflicts of interest.

References

1. Yu G, Gao J, Hummelen JC, Wudl F, Heeger AJ (1995) Polymer photovoltaic cells: Enhanced efficiencies via a network of internal donor-acceptor heterojunctions. Science 270:1789–1791
2. Hu Z, Ying L, Huang F, Cao Y (2017) Towards a bright future: polymer solar cells with power conversion efficiencies over 10%. Sci China Chem 60:571–582
3. Xiao Z, Jia X, Ding L (2017) Ternary organic solar cells offer 14% power conversion efficiency. Sci Bull 62:1562–1564
4. Li W, Ye L, Li S, Yao H, Ade H, Hou J (2018) A high-efficiency organic solar cell enabled by the strong intramolecular electron push–pull effect of the non-fullerene acceptor. Adv Mater 30:1707170
5. Chen W, Shen W, Wang H, Liu F, Duan L, Xu X, Yang R (2019) Enhanced efficiency of polymer solar cells by improving molecular aggregation and broadening the absorption spectra. Dyes Pigm 166:42–48
6. Zhang QT, Tour JM (1997) Low optical bandgap polythiophenes by an alternating donor/acceptor repeat unit strategy. J Am Chem Soc 119:5065–5066
7. Prabhu R, Roopashree B, Jeevananda T, Srilatha Rao S, Reddy KR, Raghu AV (2021) Synthesis and corrosion resistance properties of novel conjugated polymer-$Cu_2Cl_4L_3$ composites. Mater Sci Energy Technol 4:92–99
8. Dakshayinia BS, Reddyb KR, Mishrac A, Shetti NP, Malode SJ, Basu S, Naveen S, Raghu AV (2019) Role of conducting polymer and metal oxide-based hybrids for applications in amperometric sensors and biosensors. Microchem J 147:7–24
9. Prabhu R, Jeevananda T, Reddy KR, Raghu AV (2021) Polyaniline-fly ash nanocomposites synthesized via emulsion polymerization: Physicochemical, thermal and dielectric properties. Mater Sci Energy Technol 4:107–112
10. Naik MA, Raghavendra M, Siram RBK, Patil S (2013) Polymer solar cells: Design of materials by donor–acceptor approach. Curr Sci 105:1115–1123
11. Ahmed E, Subramaniyan S, Kim FS, Xin H, Jenekhe SA (2011) Benzobisthiazole-based donor–acceptor copolymer semiconductors for photovoltaic cells and highly stable field-effect transistors. Macromolecules 44:7207–7219
12. Li Z, Zhou D, Li L, Li Y, He Y, Liu J, Peng Q (2013) Synthesis and characterization of copolymers based on benzotriazoles and different atom-bridged dithiophenes for efficient solar cells. Polym Chem 4:2496–2505
13. Evenson SJ, Rasmussen SC (2010) *N*-acyldithieno [3, 2-b: 2′, 3′-d] pyrroles: second generation dithieno [3, 2-b: 2′, 3′-d] pyrrole building blocks with stabilized energy levels. Org Lett 12:4054–4057
14. Vanormelingen W, Kester J, Verstappen P, Drijkoningen J, Kudrjasova J, Koudjina S, Maes W (2014) Enhanced open-circuit voltage in polymer solar cells by dithieno [3, 2-b: 2′, 3′-d] pyrrole N-acylation. J Mater Chem A 2:7535–7545
15. Kesters J, Verstappen P, Vanormelingen W, Drijkoningen J, Vangerven T, Devisscher D, Maes W (2015) *N*-acyl-dithieno [3, 2-b: 2', 3'-d] pyrrole-based low bandgap copolymers affording improved open-circuit voltages and efficiencies in polymer solar cells. Sol Energy Mater Sol Cells 136:70–77
16. Hong D, Lv M, Lei M, Chen Y, Lu P, Wang Y, Chen X (2013) *N*-acyldithieno [3, 2-b: 2′, 3′-d] pyrrole-based low-band-gap conjugated polymer solar cells with amine-modified [6, 6]-phenyl-C61-butyric acid ester cathode interlayers. ACS Appl Mater Interfaces 5:10995–11003
17. Mai HLT, Truong NTT, Nguyen TQ, Doan BK, Tran DH, Nguyen LTT, Nguyen HT (2020) Synthesis and characterization of donor–acceptor semiconducting polymers containing 4-(4-((2-ethylhexyl) oxy) phenyl)-4 H-dithieno [3, 2-b: 2′, 3′-d] pyrrole for organic solar cells. New J Chem 44:16900–16912
18. Zou Y, Najari A, Berrouard P, Beaupré S, Réda Aïch B, Tao Y, Leclerc M (2010) A thieno [3, 4-c] pyrrole-4, 6-dione-based copolymer for efficient solar cells. J Am Chem Soc 132:5330–5331
19. Peet J, Heeger AJ, Bazan GC (2009) Plastic solar cells: Self-assembly of bulk heterojunction nanomaterials by spontaneous phase separation. Acc Chem Res 42:1700
20. Cheng YJ, Yang S, Hsu CS (2009) Synthesis of conjugated polymers for organic solar cell applications. Chem Rev 109:5868–5923
21. Thompson BC, Fréchet JM (2008) Polymer–fullerene composite solar cells. Angew Chem 47:58–77
22. Dennler G, Scharber MC, Brabec CJ (2009) Polymer-fullerene bulk-heterojunction solar cells. Adv Mater 21:1323–1338
23. Li Z, Tsang SW, Du X, Scoles L, Robertson G, Zhang Y, Ding J (2011) Alternating copolymers of cyclopenta [2, 1-b; 3, 4-b′] dithiophene and thieno [3, 4-c] pyrrole-4, 6-dione for high-performance polymer solar cells. Adv Funct Mater 21:3331–3336

24. Yuan MC, Chiu MY, Liu SP, Chen CM, Wei KH (2010) A thieno [3, 4-c] pyrrole-4, 6-dione-based donor-acceptor polymer exhibiting high crystallinity for photovoltaic applications. Macromolecules 43:6936–6938
25. Cui C, Wong WY (2016) Effects of alkylthio and alkoxy side chains in polymer donor materials for organic solar cells. Macromol Rapid Commun 37:287–302
26. Li X, Weng K, Ryu HS, Guo J, Zhang X, Xia T, Sun Y (2020) Non-fullerene organic solar cells based on benzo [1, 2-b: 4, 5-b′] difuran-conjugated polymer with 14% efficiency. Adv Funct Mater 30:1906809
27. Zhang L, Liu X, Sun X, Duan C, Wang Z, Liu X, Cao Y (2019) 4-Methylthio substitution on benzodithiophene-based conjugated polymers for high open-circuit voltage polymer solar cells. Synth Met 254:122–127
28. Li B, Zhang Q, Dai G, Fan H, Yuan X, Xu Y, Ma W (2019) Understanding the impact of side-chains on photovoltaic performance in efficient all-polymer solar cells. J Mater Chem C 7:12641–12649
29. Zhong L, Bin H, Angunawela I, Jia Z, Qiu B, Sun C, Li Y (2019) Effect of replacing thiophene by selenophene on the photovoltaic performance of wide bandgap copolymer donors. Macromolecules 52:4776–4784
30. Li X, Huang G, Jiang H, Qiao S, Kang X, Chen W, Yang R (2019) Novel benzodithiophene unit with an alkylthiobiphenyl side chain for constructing high-efficiency polymer solar cells. J Mater Chem C 7:6105–6111
31. Tan H, Tan H, Zheng X, Yang J, Yu J, Zhu W (2020) Significant influence of the benzothiophene ring substitution position on the photovoltaic performance of benzodithiophene-based donor polymers. J Mater Chem C 8:3183–3191
32. Zhang W, Mao Z, Zheng N, Zou J, Wang L, Wei C, Huang J, Gao D, Yu G (2016) Highly planar cross-conjugated alternating polymers with multiple conformational locks: Synthesis, characterization and their field-effect properties. J Mater Chem C 4:9266–9275
33. Warnan J, Labban AE, Cabanetos C, Hoke ET, Shukla PK, Risko C, Brédas JL, McGehee MD, Beaujuge PM (2014) Ring substituents mediate the morphology of PBDTTPD-PCBM bulk-heterojunction solar cells. Chem Mater 26:2299–2306
34. Raghu AV, Anita G, Barigaddi YM, Gadaginamath GS, Aminabhavi TM (2006) Synthesis and characterization of novel polyurethanes based on 2,6-Bis(4-hydroxybenzylidene) cyclohexanone hard segments. J Appl Polym Sci 104:81–88
35. Kanimozhi C, Yaacobi-Gross N, Burnett EK, Briseno AL, Anthopoulos TD (2014) Salzneret U (2014) use of side-chain for rational design of n-type diketopyrrolopyrrole-based conjugated polymers: What did we find out? Phys Chem Chem Phys 16:17253–17265
36. Manninen V, Niskanen M, Hukka TI, Pasker F, Claus S, Höger S, Baek J, Umeyama T, Imahoric H, Lemmetyinena H (2013) Conjugated donor–acceptor (D–A) copolymers in inverted organic solar cells – a combined experimental and modelling study. J Mater Chem A 2013:7451–7462